Northern Norway paleofire records reveal two distinct phases of early human impacts on fire activity

Rebecca G. Topness[a], Richard S. Vachula[a,b,c], Nicholas L. Balascio[a], William J. D'Andrea[d], Genevieve Pugsley[a], Moussa Dia[a], Martina Tingley[e], Lorelei Curtin[d], Stephen Wickler[f], R. Scott Anderson[e]

[a] Department of Geology, William & Mary, Williamsburg, VA, USA

[b] Virginia Institute of Marine Science, William & Mary, Gloucester Point, VA, USA

[c] Department of Geosciences, Auburn University, Auburn, AL, USA

[d] Lamont-Doherty Earth Observatory of Columbia University, Palisades, NY 10964, USA

[e] School of Earth and Sustainability, Northern Arizona University, Flagstaff, AZ, USA

[f] The Arctic University Museum of Norway, UiT The Arctic University of Norway, Tromsø, Norway

Corresponding authors:

Nicholas L. Balascio (nbalascio@wm.edu) and Richard S. Vachula (rsv0005@auburn.edu)

Keywords

Charcoal; Polycyclic Aromatic Hydrocarbons; Paleofire; Archaeology; Lofoten Islands; Norway

Abstract

Paleofire records document fire's response to climate, ecosystem changes, and human-activity, offering insights into climate-fire-human relationships and the potential response of fire to anthropogenic climate change. We present three new lake sediment PAH records and a charcoal record from the Lofoten Islands, Norway to evaluate the Holocene fire history of northern Norway and examine human impacts on fire in this region. All three datasets show an increase in PAH accumulation rate over the past c. 7500 cal yr BP, with an increase c. 5000 cal yr BP that signals initial human impacts on fire activity. More significant increases c. 3500 cal yr BP reach a maximum c. 2000 cal yr BP that correlates with the establishment and expansion of agricultural settlements in Lofoten during the Late Bronze Age and Pre-Roman Iron Age. Decreased PAH accumulation rates c. 1500-900 cal yr BP reflect less burning during the Late Iron Age and early medieval period. A shift toward higher molecular weight PAHs and increasing PAHs overall from c. 1000 cal yr BP to present, reflects intensified human activity. Sedimentary charcoal (>125 and 63-125 μm) in the Lauvdalsvatnet record does not vary until an increase in the last 900 years, showing a proxy insensitivity to human-caused fire. The late Holocene increase in fire activity in Lofoten follows trends in regional charcoal records, but exhibits two distinct phases of increased fire that reflect the intensity of burning due to human landscape changes that overwhelms the signal of natural variations in regional fire activity.

1. Introduction

Fire is a significant driver of environmental change and responds to changes in the climate system and human activities. Paleofire records offer a means to assess the response of fire to changing environmental conditions (Conedera et al., 2009). Distinguishing between natural and anthropogenic influences on fire regimes remains a major challenge for paleofire studies (Bowman et al., 2011; D'Anjou et al., 2012; Marlon, 2020) yet could lead to more effective forest management practices and improved preparation for future consequences of climate change (Clear et al., 2014; Marlon, 2020). However, uncertainties surrounding paleofire proxies remain and the attribution of fire occurrence to anthropogenic activities is not straightforward (Abrams and Nowacki, 2020; Oswald et al., 2020; Roos, 2020).

There are many approaches for reconstructing fire histories. Charcoal preserved in the sedimentary record and fire scars in tree rings are among the most commonly used; however, both proxies provide a predominantly local signal (on the order of 10s of kilometers; (Vachula et al., 2018)), and fire scars are limited to the age of the tree (Conedera et al., 2009; Marlon et al., 2012). Arctic sedimentary charcoal concentrations tend to be low due to the prevalence of tundra ecosystems, which burn infrequently (Hu et al., 2015), and the limited biomass available for fire relative to lower latitudes (Krawchuk et al., 2009; Pausas and Ribeiro, 2013). Likewise, although fire is more common in boreal forests, other complications like sedimentary slumps can still complicate the interpretation of charcoal records (Kelly et al., 2013). As a result, low charcoal concentrations in polar regions present a major limitation, preventing detailed fire regime characterization through traditional charcoal analysis (Chipman et al., 2015; Vachula et al., 2020). PAHs, incomplete combustion products, can also be used as a tool for reconstructing fire activity and are helping to extend the scope of paleofire research (Conedera et al., 2009; Karp et al., 2020). Polycyclic aromatic hydrocarbons (PAHs) are a group of chemical compounds characterized by fused aromatic rings produced through the burning of organic matter (Karp et al., 2020; Lima et al., 2005). Though previous studies have primarily focused on their role as pollutants originating from human activities (Andersson et al., 2014; Balmer et al., 2019; Eide et al., 2011), when used alongside charcoal records or other indicators of human activity, PAHs can provide evidence for natural and human drivers of fire regime change on a regional scale (Battistel et al., 2017; Denis et al., 2012; Tan et al., 2020), with recent research showing correlations between PAHs and area burned within 10s to 100s of kilometers (Vachula et al., 2022). Furthermore, these molecular biomarkers can preserve information about fuel source and the type of plant community burned (Karp et al., 2020; Lima et al., 2005). As charcoal and PAHs record different aspects of fire history, they are complementary proxies that can provide nuanced paleofire information.

The Holocene fire history of Fennoscandia is primarily based on charcoal and fire scar data (Clear et al., 2014; Molinari et al., 2020; Olsson et al., 2010). These data broadly reveal the relationship between fire and long-term vegetation dynamics, as well as the influence of human activities beginning in the late Holocene. However, the number of records is sparse considering the size of the region, the range of vegetation types, and regional variations in the scale of early human influences on fire. Moreover, few studies in the Fennoscandian region have applied PAHs to reconstruct more detailed aspects of fire history. D'Anjou et al. (2012) used total PAH concentrations from one site in concert with other geochemical methods to reconstruct human-driven landscape change in the Lofoten Islands. Other studies have documented PAH concentrations to better understand pollution sources in Norway (Andersson et al., 2014; Eide et al., 2011).

Here we characterize the Holocene fire history of northern Norway by developing and analyzing charcoal and PAH records from three lake sediment archives from the island of Vestvågøya, in the Lofoten Archipelago. We present trends in different charcoal size fractions and molecular distributions of PAHs. We compare these new records to previously published paleofire data to provide greater regional context for the Fennoscandian region.

2. Study Area

The Lofoten archipelago is a chain of mountainous islands extending into the Norwegian Sea off the coast of northern Norway (Figure 1). Lofoten experiences a mild climate despite its location above the Arctic Circle (67-70°N). Seasonal temperatures range from -1°C to 13°C and average monthly precipitation ranges from 40 mm in summer to 220 mm in winter. Holocene climate variations in Lofoten and nearby coastal locations follow insolation-driven trends on millennial timescales, and paleoclimate records (Balascio et al., 2020; Balascio and Bradley, 2012; Nichols et al., 2009) generally indicate moist and relatively warm conditions during the early Holocene followed by warm and dry conditions during the mid-Holocene thermal maximum c. 7000-5000 cal yr BP, followed by cooler and wetter conditions from 4000 cal yr BP to present. Early Holocene vegetation records are rare from this region, and the late Holocene record is complicated by human activities. However, vegetation changes generally follow these climate trends, with graminoids common in the early Holocene, tree birch (*Betula pubescens*) common in the middle Holocene and increasing development of wetter *Sphagnum* bog conditions after c. 4000 cal yr BP (Vorren et al., 2012).

Evidence for occupation of the Storbåhellaren rockshelter site on the island of Flakstad by c. 8000 cal yr BP represents one of the earliest records of human settlement in Lofoten (Utne, 1973). Although initial human occupation in Lofoten is likely to be significantly earlier than this date, potential settlement sites have been submerged or otherwise impacted by a mid-Holocene relative sea-level transgression. During the late Holocene, evidence for small-scale agricultural activity has been dated to c. 4200 cal yr BP (Johansen and Vorren, 1986; Vorren, 1979). An expansion of agricultural activity and the introduction of domesticated animals occurred in the Late Bronze Age c. 3100-2500 cal yr BP. The local population increased during the Iron Age (c. 2500-900 cal yr BP), marked by an increase in the number and variety of archaeological sites dating to this period (Balascio and Wickler, 2018). Many of these sites are located on Vestvågøya and are associated with the settlement at Borg, which was a chieftain center during the Late Iron Age.

The progressive increase in human-landscape interactions during the late Holocene has been documented by pollen data from local bogs (Johansen and Vorren, 1986; Tingley, 2022; Vorren, 1979; Vorren et al., 2012) and organic geochemical changes based on a lake sediment record from Lilandsvatnet (68°13'59"N 13°45'29"E) (D'Anjou et al., 2012). Changes in landscape burning associated with natural forest fires and human activities were explored by D'Anjou et al. (2012) who documented a significant increase in PAHs c. 2250 cal yr BP. However, questions remain as to whether these trends reflect catchment-specific landscape changes or broader regional trends. Here we explore the region's fire history in greater detail through the analysis of PAHs in sediment records from three different catchment settings, by studying trends in total

PAHs and relative abundance of individual PAH compounds, and by developing a local charcoal record.

The paleofire records were generated from sediment cores from three sites on Vestvågøya near Borg (Figure 1). We analyzed cores from the lake Ostadvatnet (4.6 km^2; 68°13'31" N, 13°42'40" E), which is within the main agricultural valley on Vestvågøya, and the lake Lauvdalsvatnet (2.7 km^2; 68°14'07" N, 13°54'22" E), located within a narrow upland valley southeast of Borg. We also developed a record from Inner Borgpollen (15.2 km^2, 68°14'53" N, 13°48'56" E), a restricted marine basin that served as a harbor for the Iron Age settlement at Borg (Balascio and Wickler, 2018).

3. Materials and methods

3.1 Core collection and analysis

Sediment cores were collected from each site in plastic tubes using a Uwitec gravity corer or a percussion coring device, which were then packaged in the field and transported to the laboratory for analysis. A 176-cm gravity core (IND-01-17) was recovered from Inner Borgpollen, and a 132.5-cm gravity core (OSD-02-17) was recovered from Ostadvatnet, both with intact sediment-water interfaces. A 241.5-cm composite record was developed for Lauvdalsvatnet using a 221-cm percussion core (LVP-01-17) and a 40-cm gravity core (LVD-01-17). Magnetic susceptibility profiles and radiocarbon ages were used to align the stratigraphy of the cores. General paleoenvironmental conditions were initially characterized by generating total carbon and carbon/nitrogen (C/N) profiles for each record. Samples were freeze-dried, ground, and 4-6 mg aliquots were analyzed using an Elementar vario MICRO cube element analyzer.

3.2 Chronologies

Radiocarbon dating was performed on plant macrofossils picked from core surfaces (Table 1). Analyses were conducted at the University of California, Irvine, Keck Carbon Cycle AMS Laboratory (UCI) and at the National Ocean Sciences AMS Laboratory at Woods Hole Oceanographic Institution (OS). Dates were calibrated to calendar years before AD 1950 (cal yr BP) using CALIB version 8.20 (Stuiver and Reimer, 1993) with the IntCal20 calibration dataset (Reimer et al., 2020). Age-depth models were created for each core using the Bacon age-modelling software in R (Blaauw and Christen, 2011).

3.3. PAH Analysis

We analyzed lipids extracted from the Lauvdalsvatnet, Ostadvatnet, and Inner Borgpollen sediment core samples. Lipids were extracted from freeze-dried samples with 9:1 (v:v) dichloromethane:methanol using a Dionex Accelerated Solvent Extractor (ASE 350). Silica gel column chromatography was used to divide the TLE phase into three fractions with solvents of increasing polarity as follows: (F1) hexane, (F2) dichloromethane, (F3) methanol. The F2 fractions were analyzed using an Agilent 7890A gas chromatograph coupled with a 5975 mass selective detector. The gas chromatograph was equipped with a DB-5MS capillary column (30 m length, 320 µm outer diameter, and 0.25 µm film thickness). Sedimentary PAHs were quantified using select ion monitoring (SIM) mode and by comparison with an external calibration curve (Sigma-Aldrich CRM47940). The calibration curve was established by measuring the response factors of each target ion for a range of known dilutions (n=5) of the PAH standard. The calibration curve was re-established every 25 samples. Re-establishments of the calibration curve doubled as a means to ensure limited instrumental drift across sample runs. Individual calibration curves were established for each PAH due to the variable response between each compound. Sixteen PAHs were quantified: naphthalene (Na), acenaphthylene (Ayl), acenaphthene (Ace), fluorene (Fl), anthracene (An), phenanthrene (Phe), fluoranthene (Fla), pyrene (Py), benz[a]anthrene (Ba), chrysene (Ch), retene (Ret), benzo[k]fluoranthene (BkF), benzo[a]pyrene (BaP), benzo[g,h,i]perylene (Bghi), dibenzo[a,h]anthracene (DiAn), and ideno[1,2,3-cd]pyrene (IP). A compound persistently coeluted with benzo[b]fluoranthene (BbF) during SIM mode and could not be distinguished or isolated, so we did not quantify BbF. PAH accumulation rates (as opposed to fluxes or mass accumulation rates) were determined using the age-depth models of the sediment cores. Our use of accumulation rates eliminates the potential influence of sediment density changes biasing our PAH interpretations.

To group our PAH data, we defined low molecular weight (LMW) PAHs as those with 2-3 rings and a molecular weight less than or equal to 200 g/mol: Na, Ayl, Ace, Fl, An, and Phe. Compounds with 4-6 rings and a molecular weight greater than 200 g/mol were considered high molecular weight (HMW) PAHs: Fla, Py, Ba, Ch, Ret, BkF, BaP, Bghi, DiAn, and IP (Lima et al., 2005). We use these LMW and HMW groupings when presenting our data, but subset our data to mimic the groupings used in previous research for direct comparability when necessary (e.g., for the LMW/Total value (Karp et al., 2020)). The ratio of low molecular weight to total

PAHs (LMW/Total; wherein LMW = Phe + An + Fl + Py, and Total = Phe + An + Fl + Py + Ba + Ch + BkF + BaP + IP + Bghi) was used to interpret distance transported from the source and PAH burn phase (Karp et al., 2020).

3.4 Charcoal Analysis

Charcoal was analyzed in the core from Lauvdalsvatnet to complement the PAH data and to more directly compare to regional charcoal records compiled for Fennoscandia. Lauvdalsvatnet was chosen because of its small size, steep surrounding slopes, and relatively large watershed area. These watershed characteristics are more likely to concentrate charcoal than the large lake areas and gently sloping watersheds of Ostadvatnet and Inner Borgpollen (Whitlock and Larsen, 2002).

For charcoal analysis, 0.5 cm^3 samples were taken every 10-cm (n = 28 samples). The samples were soaked in a 50:50 mixture of 10% bleach and sodium hexametaphosphate. After 48 hours, the samples were sieved through nested 63 μm and 125 μm sieves with deionized water. Charcoal particles were quantified in gridded petri dishes using a binocular dissecting microscope. The particles were distinguished from inorganic particles by several characteristics: particles that were vitreous, black, and opaque with identifiable vegetal structures were counted (Whitlock and Larsen, 2002). Identifying characteristics included observable plant fragments and structures, such as stomata and cellular walls, as well as particles that had low densities and moved easily in the slide. Charcoal accumulation rates (CHAR, # particles cm^{-2} yr^{-1}) were estimated using the volumetric concentration and the age-depth model for the record (Vachula et al., 2018).

4. Results

4.1 Sediment stratigraphy and chronologies

Stratigraphic and chronologic data show that each record contains sediment sequences without any significant sedimentation rate or compositional changes over the last 7600 cal yr BP (Figure 2 and 3). The Ostadvatnet core consists of homogenous, fine-grained, dark brown, organic-rich sediment with faint bands of lighter brown intervals. The age-depth model is based on three radiocarbon ages and shows the core has a basal age of c. 6100 cal yr BP with an average sedimentation rate of 0.22 mm/yr. Total carbon values generally fluctuate around a mean of 11% and C/N values range from 11 to 9, indicating organic matter is primarily from aquatic sources (Figure 3). Sediments from Inner Borgpollen are dark brown to black, organic-rich, and with faint layering. The sediments get darker and more strongly layered towards the top of the record. An age-depth model was developed for the Inner Borgpollen record using six radiocarbon ages and shows that the core has a basal age of 3500 cal yr BP with an average sedimentation rate of 0.5 mm/yr (Figure 2). Total carbon values average c. 12% from 3500 to 500 cal yr BP and increase to c. 15% over the last 500 years. C/N values are more stable with an average of 11 (Figure 3). The Lauvdalsvatnet record contains two lithostratigraphic units. The basal unit (224-241.5 cm) is a gray, poorly sorted coarse sand with some pebbles, likely due to a mass movement in the catchment. We focus on the fine-grained uppermost sediments, above 241.5 cm, which are generally dark brown, organic rich and with some lighter minerogenic layers throughout. The age-depth model for Lauvdalsvatnet is defined by six radiocarbon ages and shows that the record has a basal age of c. 7600 cal yr BP at 241.5 cm and an average sedimentation rate is 0.32 mm/yr (Figure 3). Total carbon values fluctuate around an average of 11% with no significant trends, and C/N values average at 13 with a slight increasing trend after c. 6000 cal yr BP.

4.2 Polycyclic Aromatic Hydrocarbons (PAHs)

Total PAH concentrations in samples analyzed from Inner Borgpollen, Ostadvatnet, and Lauvdalsvatnet range from 0.46 to 4.62 μg/g of dry sediment (Figure 4). HMW compounds are generally more abundant than LMW compounds. Benzo[k]fluoranthene is the most abundant at each site, and among LMW compounds, anthracene has the highest concentration at all three sites. Total PAH concentrations vary among the sites and are highest in Lauvdalsvatnet and lowest in Ostadvatnet.

The total PAH (sum of the 16 PAHs) accumulation rates are very similar among the three lake sediment records and show an increase in accumulation rates over the past 7500 cal yr BP, ranging from 0 to 46.3 ng/g/yr (Figure 5A). The mid-Holocene (7500-5000 cal yr BP) is characterized by PAH levels that are below the detection limits for samples from Lauvdalsvatnet and Ostadvatnet. This interval is followed by an abrupt increase in PAH accumulation rate at c. 5000 cal yr BP that reaches a maximum c. 2000 cal yr BP. Values decrease until 1000 cal yr BP, and the last 1000 years is characterized by increasing accumulation rates. The highest values at all three sites are within the last 200 years. A five-point running average of the PAH data from all three records highlights the two intervals of higher PAH accumulation rates from c. 2400-1600 cal yr BP and 900 cal yr BP to present.

Among the individual sites, similar trends in PAHs are visible with modest differences (Figure 5A). PAH data from Inner Borgpollen record some of the lowest and highest PAH accumulation rates, ranging from 0 to 46.3 ng/g/yr. Values are low (less than 1 ng/g/yr) but increase throughout the majority of the record (3400-1400 cal yr BP). An abrupt increase in values c. 1000 cal yr BP continued to the present, reaching the highest values of the record in modern sediments. In contrast, the Ostadvatnet record has relatively low, fluctuating values that abruptly increased and reached a maximum c. 2000 cal yr BP. PAH accumulation rate then declined before increasing again in the most recent 500 years. Ostadvatnet has the lowest overall accumulation rate, ranging from 0 to 1.10 ng/g/yr. The Lauvdalsvatnet data closely resemble trends seen in the Ostadvatnet data, but with more variability. Accumulation rates range from 0 to 20.5 ng/g/yr. The interval from 7500-5000 cal yr BP is characterized by PAH concentrations below detection limits. Low PAH accumulation (less than 1 ng/g/yr) occurred from 5000 to 2500 cal yr BP. This interval was followed by increasing values that reached a maximum c. 2000 cal yr BP, as for the other two records. This maximum was followed by fluctuating, declining values until 1000 cal yr BP when values began to increase through the remainder of the record, reaching values similar to Inner Borgpollen.

The PAH data were further grouped by low molecular weight (LMW) and high molecular weight (HMW) for all three sites (Figure 5B,C). Trends in the accumulation rates of HMW and LMW compounds are similar to total PAHs and display higher values from c. 2400-1600 cal yr BP and

900 cal yr BP to present. HMW compounds are generally more abundant and show a more pronounced increase over the last 1000 years. Interestingly, significant shifts in the relative abundance of HMW and LMW PAHs were observed in Lauvdalsvatnet (Figure 6A,B). From 3500-1000 cal yr BP, LMW PAHs are significantly more abundant in Lauvdalsvatnet. This shift in the accumulation of LMW PAHs is characterized by fluctuating trends with dominant peaks c. 2000 cal yr BP and c. 700 cal yr BP. Over this interval, LMW PAHs range from 0 and 0.867 ng/g/yr. Meanwhile, accumulation of HMW PAHs mirrors these trends. After 2000 cal yr BP, the accumulation rate of HMW PAHs began to fluctuate with values ranging from 0 to 20.03 ng/g/yr, reaching a peak at approximately 100 cal yr BP while LMW PAHs decline.

4.3 Lauvdalsvatnet Charcoal

Charcoal accumulation rates (CHAR) were quantified for the >125 μm and 63-125 μm size fractions for the past c. 7500 cal yr BP in Lauvdalsvatnet (Figure 6C). Both size fractions exhibit generally steady values throughout the record: particles greater than 125 μm have an average accumulation rate of 0.193 particles cm^{-2} yr^{-1} and particles between 63-125 μm have an average accumulation rate of 0.788 particles cm^{-2} yr^{-1}. From c. 7500 to 2000 cal yr BP, the record shows low, fluctuating values. After 1000 cal yr BP, charcoal accumulation rates significantly increased toward the present day. Accumulation rates for CHAR >125 μm and CHAR 63-125 μm are positively correlated (r = 0.58). Correlations between CHAR values of the two size fractions also appear to have varied through time (Figure 6D). Correlation coefficients using a 5-point window show a period of sustained inversely correlated values from c. 3000-1500 cal yr BP and a sustained period of positively correlated values from 1500 cal yr BP to present. These trends in correlations are interesting and may reflect paleofire dynamics, however the correlations are not statistically significant due to the small sample size.

5. Discussion

5.1 Interpreting paleofire proxies

PAH and charcoal data from Lauvdalsvatnet, Ostadvatnet, and Inner Borgpollen provide detailed paleofire information for the Lofoten Islands over the last c. 7500 cal yr BP. Total PAH accumulation data are sensitive indicators for changes in overall fire activity (Andersson et al., 2014; Balmer et al., 2019; Karp et al., 2020; Tan et al., 2020). We also differentiate trends in LMW and HMW compounds that have previously been used to infer combustion phase (i.e., smoke vs. particulate), which has implications for understanding the pathways and mechanisms of PAH transport from source fires (Karp et al., 2020). Karp et al. (2020) found that PAHs derived from smoke and combustion residues exhibit LMW/Total values of 0.35-0.8 and 0.75-0.95, respectively. We therefore interpret a LMW/Total value of 0.75 as a general cut-off between smoke and combustion residues. For example, LMW/Total PAH values from 5000-3500 cal yr BP are characteristic of combustion residues (<0.75), while values from 3500-1000 cal yr BP (>0.75) fall in the range that characterizes smoke phasing.

Charcoal data from Lauvdalsvatnet complement our PAH records and allow direct comparison to previously published paleofire records from Fennoscandia. We analyzed different charcoal size fractions, which can be used to distinguish local from more regional fire activity (Gardner and

Whitlock, 2001; Vachula et al., 2019). Charcoal particles > 125 µm better represent local fire activity, whereas smaller particles (63-125 µm), which can be transported farther from the source, and can better record regional fire activity (Gardner and Whitlock, 2001; Higuera et al., 2011; Vachula et al., 2018). Previous research has shown that these size fractions reliably reflect area burned within ~35 and ~150 km, respectively (Vachula et al., 2018), though there is always some variability between sites (Vachula, 2021). We therefore interpret the >125 µm size fraction to reflect fire activity near the Borg settlement and on Vestvågøoya whereas the 63-125 size fraction likely records fire in the broader Lofoten Archipelago and mainland Fennoscandia. Correlations between charcoal size fractions can therefore be used to investigate relationships between local and regional fire activity. Highly correlated values have been interpreted to reflect a state of more natural fire activity rather than a human-perturbed fire regime (Vachula et al., 2019) based on observations that wildfire tends to be self-similar across spatial scales (Malamud et al., 1998; Turcotte and Malamud, 2004), but that anthropogenic impacts impede this continuity. Together, PAH and charcoal datasets inform our understanding of local and regional burning related to natural and anthropogenic activities and define specific paleofire intervals.

5.2 Fire History of the Lofoten Islands

The fire history of Lofoten based on data from Lauvdalsvatnet, Ostadvatnet, and Inner Borgpollen can be divided into three distinct phases (Figure 5). These phases are primarily defined by trends in PAHs, which are similar among the three sites. The similarity in trends is remarkable considering differences in catchment size (ranging from 2.7 to 15.2 km^2), geographic setting, and water column properties of each lake, which are factors that could influence delivery, transport, or preservation of PAHs. Characteristics of these phases in paleofire activity are also supported by charcoal data from Lauvdalsvatnet.

Prior to c. 5000 cal yr BP, PAH levels in the sediments were below detection limits, and there are low CHAR values at Lauvdalsvatnet for both size fractions from 7500 to 5500 cal yr BP (Figure 5, 6), indicating that fires were not abundant in the region. At c. 5000 cal yr BP, detectable PAH concentrations are first measured in Ostadvatnet and Lauvdalsvatnet, and based on data from all three lakes, PAHs accumulation increased c. 2400 cal yr BP and reached maximum accumulation rates c. 2000 cal yr BP (Figure 5). This increase is accompanied by a distinct shift c. 3500 cal yr BP in the composition of PAHs towards LMW compounds, which is indicative of a shift to smoke phase. Smoke PAHs tend to be low molecular weight and associated with lower combustion temperatures (Karp et al., 2020; McGrath et al., 2003), so this shift could reflect a change towards lower intensity, potentially anthropogenic fires. CHAR values for both size fractions remain low through this interval (c. 5000-2000 cal yr BP) showing an insensitivity of this proxy to low combustion temperature fires inferred from PAHs. Others have found that low-intensity fires are poorly represented in sedimentary charcoal records (Higuera et al., 2005), potentially as a function of methodological biases (Constantine IV and Mooney, 2021). The lack of response in CHAR values at our sites is also possibly a result of limited charcoal production and/or atmospheric transport from this type of burning in this environment, as lower temperature fires provide less convective energy to mobilize the dispersal of charcoal (Clark, 1988; Peters and Higuera, 2007; Vachula and Richter, 2018). The sustained interval of inversely correlated charcoal size fractions from 3000 to 1500 cal yr BP is noteworthy and may also suggest human impacts on fire and land use based on the interpretation that they indicate a disconnect between local and regional burning.

We interpret these trends in our paleofire data to indicate that humans began to impact the fire regime of Lofoten c. 3500 cal yr BP, although initial human impacts on fire activity could have begun as early as 5000 cal yr BP. More significant landscape burning is evident after c. 2400 cal yr BP. It is unlikely that these changes can be explained by climatic factors, as paleoclimate data suggest Lofoten and northern Norway experienced a general shift to cooler and wetter conditions during the late Holocene (Bakke et al., 2008; Balascio et al., 2020; Balascio and Bradley, 2012). Moreover, previous work has shown that human activities increased the occurrence of fire in Fennoscandia beginning c. 3,000 years BP (Clear et al., 2014). This increase has been attributed to the expansion of permanent settlements and use of slash and burn agriculture that lasted until 500-300 years BP, when there was a transition from slash and burn techniques to modern agriculture and forestry characterized by fire suppression (Clear et al., 2014; Molinari et al., 2020). In northern Norway, a similar timing for a regional expansion in agricultural has been documented with pollen data (Sjögren and Arntzen, 2013). In Lofoten, the expansion of agricultural activity, from small-scale pioneering settlements, began during the Late Bronze Age c. 3100-2500 cal yr BP and continued into the Early Iron Age (c. 2500-1400) (Balascio and Wickler, 2018; Johansen and Vorren, 1986; Vorren et al., 2012). The timing of these early changes in our paleofire data corresponds well with evidence from Lofoten and the distinct increasing trend in PAHs likely reflects agricultural expansion associated with initial forest clearance. The paleofire record from Lilandsvatnet in Lofoten based on PAHs (though only Fla, Py, BeP, Bghi, and picene) also shows an abrupt increase at a similar time, c. 2250 cal yr BP, which corresponds with a sharp transition from forest to grassland in the same record, as interpreted from trends in leaf wax compositions (D'Anjou et al., 2012) (Figure 7C).

Following the onset of human impacts on the fire regime of Lofoten and a peak in burning c. 2000 cal yr BP, there was an interval of lower PAH accumulation rates (c. 1500 – 900 cal yr BP) showing a decline in local fire activity. This interval corresponds with the Late Iron Age (c. 1450-900 cal yr BP) and the decline may reflect less burning following the initial forest clearance, when pollen data show decreasing tree pollen and increasing grasses (Anderson et al., unpublished; Tingley, 2022; Vorren, 1979). Less burning could also indicate a reduction in local farming activity, which is suggested by local pollen data grasses (Anderson et al., unpublished; Tingley, 2022; Vorren, 1979). This interval is not as well expressed in PAH data from Lilandsvatnet, which could be attributed to the different number of PAH compounds analyzed and/or catchment specific influences on PAHs accumulation rates (D'Anjou et al., 2012) (Figure 7C).

The last 900 years in our paleofire data is characterized by a distinct increase in PAHs at all three sites, and both PAH accumulation rates and CHAR values reach the highest values of the record. Locally, a dramatic increase in burning is likely associated with more widespread and intensive anthropogenic influences on landscapes. Following the Iron Age, during the medieval period, land use patterns intensified significantly and continued toward present with subsequent introductions of modern intensive farming methods. More recently, these records could be influenced by regional expansion and industrialization in northern Europe. This interval is also characterized by a shift in the composition of PAHs that is marked by a decline in the proportion of LMW PAHs relative to HMW PAHs. The increased relative abundance of HMW PAHs indicates sources from residues and/or associated with higher combustion temperatures, both of which can be attributed to more intensive anthropogenic activity and are characteristic of recent PAHs also observed in a site in western Norway (Andersson et al., 2014).

5.3 Fire in Fennoscandia

The Holocene fire history of Fennoscandia has primarily been assessed through the analysis of sedimentary charcoal records (Brown and Giesecke, 2014; Carcaillet et al., 2012; Clear et al., 2014; Molinari et al., 2020; Olsson et al., 2010; Pitkänen et al., 2002; Tryterud, 2003). Many of these studies have found that the fire sensitivity of different vegetation types is likely to have been the primary control on Holocene trends in regional fire activity. A recent study compiled 69 charcoal records and examined trends in z-scores of transformed CHAR values (Molinari et al., 2020) (Figure 7B). Their data show increasing values from c. 11,000-7,300 cal yr BP, a decreasing trend during the mid-Holocene from c. 7,300-4,600 cal yr BP, followed by increasing values from c. 4,600 cal yr BP to 500 cal yr BP, when they reach their maximum. Despite this sustained increasing trend during the late Holocene, values do not exceed the long term mean until 1,600 cal yr BP. After 500 cal yr BP values decline to present. These trends in charcoal data were compared with changes in dominant vegetation types during the Holocene based on pollen data and grouped by their fire sensitivity. They found strong positive correlations between trends in burning throughout Fennoscandia and fire-prone vegetation (e.g. Ericaceae, *Pinus*, *Betula* and *Populus*) and negative correlations with fire-intolerant taxa (e.g., *Picea*, *Ulmus Tilia*, *Fraxinus*), aside for the last millennia when human activities impacted these relationships (Molinari et al., 2020).

Paleofire data from Lofoten do not completely agree with the trends of this regional compilation. CHAR data from Lauvdalsvatnet, which are most directly comparable, do not show any significant changes from 7500-2000 cal yr BP (Figure 6). Specifically, there is not an increasing trend in CHAR values in Lauvdalsvatnet during the late Holocene, which Molinari et al. (2020) attribute to a regional increase in fire-prone vegetation. The lack of correspondence between data from Lauvdalsvatnet and the regional trend can be attributed to differences in the vegetation history of Lofoten (Tingley, 2022; Vorren, 1979). In particular, pollen from fire-prone species such as Ericaceae, *Populus*, and *Pinus* are uncommon at Lofoten sites throughout the Holocene. Moreover, arboreal birch, which has been more common, does not show an increasing trend during the late Holocene. The maritime climate of Lofoten also likely suppressed natural fires as compared to the more interior and southern sites that dominate the regional compilation. Similarities between Lauvdalsvatnet CHAR values and the regional compilation do occur in the last 1000 years, when both display their highest values, which Molinari et al. (2020) attribute to human activities and modification of natural fire-vegetation interactions.

PAH records from Lofoten are more similar to the regional charcoal compilation by Molinari et al. (2020) in that they do exhibit a general increasing trend over the late Holocene (Figure 7). However, as discussed above, local vegetation changes are unlikely to be the driver of these PAH trends. The correspondence between the PAH data and the regional charcoal compilation could reflect how PAHs record a spatially broader range of fire history than charcoal. Although recent research has shown that PAHs can be correlated to area burned at several spatial scales within 150 km (Vachula et al., 2022), there is also clear documentation that PAHs can be transported much more broadly (Halsall et al., 2001; Killin et al., 2004). So, it is possible that the Lofoten PAH data reflect the same fires recorded in the regional charcoal compilation. However, the rapid fluctuations with two distinct peaks and the evidence for changes in the intensity of fires show that early human activities starting c. 3500 cal yr BP were likely impacting the local fire regime and a dominant control of paleofire trends in Lofoten.

Overall, the Lofoten paleofire records do exhibit some of the characteristics of the compilation of charcoal data from Fennoscandia. However, the PAH records from Lofoten show a sharp increase in fire activity over the last c. 2400 years, aside from a brief decline c. 1500-900 cal yr BP, that deviates from the gradual rise in the regional compilation showing that human activities overwhelm natural fire variations. We interpret the onset of these late Holocene variations to reflect the increase in landscape burning and agricultural activity in Lofoten beginning in the Late Bronze Age. The abrupt changes in the PAH records may also reflect the greater sensitivity of PAHs, as compared to charcoal, in recording paleofire in this region. Our data also reveal two distinct intervals of increased fire activity (c. 2400-1500 cal yr BP and 900 cal yr BP-present) providing greater detail on the nature and timing of early human impacts on fire. This work emphasizes the significance and intensity of early human-landscape interactions as Lofoten developed from an agricultural outpost to an important settlement center during the Late Iron Age.

6. Conclusion

Here we present a comprehensive assessment of the Holocene paleofire history in northern Norway. Fire history was reconstructed using multiple PAH records and a charcoal record from the Lofoten Islands. These data were evaluated in the context of past human-landscape changes and the regional fire history in Fennoscandia via a compilation of published charcoal records. Our results define when humans first began to impact local patterns of fire and reveal two distinct phases of increased fire activity that we attribute to prehistoric human-landscape interactions. The trends in fire history we observe in Lofoten differ from those inferred from regional charcoal data and demonstrate the sensitivity of PAHs to detect variations in fire activity and the influence of humans that overprints natural fire variations.

Our data show evidence that humans altered local fire activity starting c. 3500 cal yr BP and more significantly after c. 2400 cal yr BP, though initial human impacts on fire activity could have begun as early as 5000 cal yr BP. All three sites (Lauvdalsvatnet, Ostadvatnet, and Inner Borgpollen) record an overall increase in total PAH accumulation rate over the past 5000 cal yr BP with much greater values within two distinct phases, c. 2400-1500 cal yr BP and 900 cal yr BP-present. The first phase of increased fire activity is characterized by increased PAH accumulation rates, PAH compositions with greater LMW compounds indicative of smoke and low intensity burning, and no significant changes in CHAR values. These trends reflect the initial establishment and expansion of agricultural settlements in Lofoten starting in the Late Bronze Age and into the Iron Age. A period of reduced fire activity follows this interval (1500-900 cal yr BP) and could indicate a decrease in fuel availability following the interval of significant land clearance and/or a reduction in local farming activity during the Late Iron Age. The second phase of increased burning (900 cal yr BP-present) is characterized by the highest PAH accumulation rates, an increase in CHAR >125 μm and CHAR 63-125 μm in Lauvdalsvatnet, and a shift to HMW PAH compositions. This phase represents the intensification of human-landscape impacts with introductions of modern intensive farming methods and the possible influence of more regional industrialization throughout northern Europe with PAH sources possibly from residues and/or associated with higher combustion temperatures.

Comparison of paleofire proxies among our Lofoten sites and to charcoal data from throughout Fennoscandia offers insights for fire reconstructions. In particular, our data show the sensitivity of PAHs, as compared to charcoal, in detecting early human impacts on burning. In Lofoten, significant increases in PAH accumulation rates occur at least 3,600 years before changes in CHAR values for charcoal particle sizes >125 μm and 63-125 μm. PAHs likely reflect smoke phases from low intensity burning, which may not produce abundant charcoal and/or transport charcoal long distances. CHAR values only seem to respond to the more significant increases in local/regional burning, and likely with higher temperature combustion, over the last 900 years. The lack of sensitivity in charcoal records is also demonstrated in trends observed in a regional compilation of charcoal datasets, which only shows a slight increase in charcoal accumulation rates over the last 2,000 years. The different responses between these proxies might be particular to this region, where natural forest fires are limited, but may offer insight in comparing these processes in other environments.

Acknowledgements

This work was supported by National Science Foundation (NSF) Grant OPP-1504270 to NLB and WJD, and NSF grant EAR-1660309 to NLB. RSV was supported by a William & Mary (W&M) Environment and Sustainability Mellon Postdoctoral Fellowship. MD was supported with a W&M Charles Center Undergraduate Research Honors Fellowship, and GP was supported with a W&M Geology Ellen Stofan Scholarship. We thank Marion Fjelde Larsen, Director of the Lofotr Viking Museum for assistance with field logistics; Elizabeth Canuel for help with data analysis; Yanhua Feng, Lee DePue, and Chloe Lund for assistance in the laboratory.

References

Abrams MD and Nowacki GJ (2020) Native American imprint in palaeoecology. *Nature Sustainability*. Nature Publishing Group 3(11): 896–897.

Andersson M, Klug M, Eggen OA and Ottesen RT (2014) Polycyclic aromatic hydrocarbons (PAHs) in sediments from lake Lille Lungegårdsvannet in Bergen, western Norway; appraising pollution sources from the urban history. *Science of the total environment*. Elsevier 470: 1160–1172.

Bakke J, Lie Ø, Dahl SO, Nesje A and Bjune AE (2008) Strength and spatial patterns of the Holocene wintertime westerlies in the NE Atlantic region. *Global and Planetary Change*. Elsevier 60(1–2): 28–41.

Balascio NL, Anderson RS, D'Andrea WJ, Wickler S, D'Andrea RM and Bakke J (2020) Vegetation changes and plant wax biomarkers from an ombrotrophic bog define hydroclimate trends and human-environment interactions during the Holocene in northern Norway. *The Holocene*. SAGE Publications Sage UK: London, England 30(12): 1849–1865.

Balascio NL and Bradley RS (2012) Evaluating Holocene climate change in northern Norway using sediment records from two contrasting lake systems. *Journal of Paleolimnology*. Springer 48(1): 259–273.

Balascio NL and Wickler S (2018) Human–environment dynamics during the Iron Age in the Lofoten Islands, Norway. *Norsk Geografisk Tidsskrift-Norwegian Journal of Geography*. Taylor & Francis 72(3): 146–160.

Balmer J, Hung H, Yu Y, Letcher R and Muir D (2019) Sources and environmental fate of pyrogenic polycyclic aromatic hydrocarbons (PAHs) in the Arctic. Emerg Contam 5: 128–142. .

Battistel D, Argiriadis E, Kehrwald N, Spigariol M, Russell JM and Barbante C (2017) Fire and human record at Lake Victoria, East Africa, during the Early Iron Age: Did humans or climate cause massive ecosystem changes? *The Holocene*. SAGE Publications Sage UK: London, England 27(7): 997–1007.

Berger A and Loutre M-F (1991) Insolation values for the climate of the last 10 million years. *Quaternary Science Reviews*. Elsevier 10(4): 297–317.

Blaauw M and Christen JA (2011) Flexible paleoclimate age-depth models using an autoregressive gamma process. *Bayesian analysis*. International Society for Bayesian Analysis 6(3): 457–474.

Bowman DMJS, Balch J, Artaxo P, Bond WJ, Cochrane MA, D'Antonio CM, et al. (2011) The human dimension of fire regimes on Earth. *Journal of Biogeography*. Blackwell Publishing Ltd 38(12): 2223–2236: doi:10.1111/j.1365-2699.2011.02595.x.

Brown KJ and Giesecke T (2014) Holocene fire disturbance in the boreal forest of central S weden. *Boreas*. Wiley Online Library 43(3): 639–651.

Carcaillet C, Hörnberg G and Zackrisson O (2012) Woody vegetation, fuel and fire track the melting of the Scandinavian ice-sheet before 9500 cal yr BP. *Quaternary Research*. Cambridge University Press 78(3): 540–548.

Chipman ML, Hudspith V, Higuera PE, Duffy PA, Kelly R, Oswald WW, et al. (2015) Spatiotemporal patterns of tundra fires: late-Quaternary charcoal records from Alaska. *Biogeosciences*. Copernicus GmbH 12(13): 4017–4027: doi:10.5194/bg-12-4017-2015.

Clark JS (1988) Particle motion and the theory of charcoal analysis: Source area, transport, deposition, and sampling. *Quaternary Research*. Elsevier 30(1): 67–80: doi:10.1016/0033-5894(88)90088-9.

Clear JL, Molinari C and Bradshaw RH (2014) Holocene fire in Fennoscandia and Denmark. *International Journal of Wildland Fire*. CSIRO Publishing 23(6): 781–789.

Conedera M, Tinner W, Neff C, Meurer M, Dickens AF and Krebs P (2009) Reconstructing past fire regimes: methods, applications, and relevance to fire management and conservation. *Quaternary Science Reviews* 28(5–6): 555–576: doi:10.1016/j.quascirev.2008.11.005.

Constantine IV M and Mooney S (2021) Widely used charcoal analysis method in paleo studies involving NaOCl results in loss of charcoal formed below 400 C. *The Holocene*. SAGE Publications Sage UK: London, England 09596836211041740.

D'Anjou RM, Bradley RS, Balascio NL and Finkelstein DB (2012) Climate impacts on human settlement and agricultural activities in northern Norway revealed through sediment biogeochemistry. *Proceedings of the National Academy of Sciences of the United States of America*. National Academy of Sciences 109(50): 20332–7: doi:10.1073/pnas.1212730109.

Denis EH, Toney JL, Tarozo R, Scott Anderson R, Roach LD and Huang Y (2012) Polycyclic aromatic hydrocarbons (PAHs) in lake sediments record historic fire events: Validation using HPLC-fluorescence detection. *Organic Geochemistry* 45: 7–17: doi:10.1016/j.orggeochem.2012.01.005.

Eide I, Berg T, Thorvaldsen B, Christensen GN, Savinov V and Larsen J (2011) Polycyclic aromatic hydrocarbons in dated freshwater and marine sediments along the Norwegian coast. *Water, Air, & Soil Pollution*. Springer 218(1): 387–398.

Gardner JJ and Whitlock C (2001) Charcoal accumulation following a recent fire in the Cascade Range, northwestern USA, and its relevance for fire-history studies. *The Holocene*. Sage Publications Sage CA: Thousand Oaks, CA 11(5): 541–549.

Halsall CJ, Sweetman AJ, Barrie LA and Jones KC (2001) Modelling the behaviour of PAHs during atmospheric transport from the UK to the Arctic. *Atmospheric Environment* 35(2): 255–267: doi:10.1016/S1352-2310(00)00195-3.

Higuera PE, Sprugel DG and Brubaker LB (2005) Reconstructing fire regimes with charcoal from small-hollow sediments: a calibration with tree-ring records of fire. *The Holocene*. Sage Publications Sage CA: Thousand Oaks, CA 15(2): 238–251.

Higuera PE, Whitlock C and Gage JA (2011) Linking tree-ring and sediment-charcoal records to reconstruct fire occurrence and area burned in subalpine forests of yellowstone National Park, USA. *Holocene*. Sage Publications Sage UK: London, England 21(2): 327–341: doi:10.1177/0959683610374882.

Hu FS, Higuera PE, Duffy P, Chipman ML, Rocha AV, Young AM, et al. (2015) Arctic tundra fires: natural variability and responses to climate change. *Frontiers in Ecology and the Environment* 13(7): 369–377: doi:10.1890/150063.

Johansen OS and Vorren K-D (1986) The prehistoric expansion of farming into "Arctic" Norway: a chronology based on 14C dating. *Radiocarbon*. Cambridge University Press 28(2A): 739–747.

Karp AT, Holman AI, Hopper P, Grice K and Freeman KH (2020) Fire distinguishers: Refined interpretations of polycyclic aromatic hydrocarbons for paleo-applications. *Geochimica et Cosmochimica Acta*. Elsevier 289: 93–113.

Kelly R, Chipman ML, Higuera PE, Stefanova I, Brubaker LB and Hu FS (2013) Recent burning of boreal forests exceeds fire regime limits of the past 10,000 years. *Proceedings of the National Academy of Sciences of the United States of America* 110(32): 13055–60: doi:10.1073/pnas.1305069110.

Killin RK, Simonich SL, Jaffe DA, DeForest CL and Wilson GR (2004) Transpacific and regional atmospheric transport of anthropogenic semivolatile organic compounds to Cheeka Peak Observatory during the spring of 2002. *Journal of Geophysical Research: Atmospheres* 109(D23): doi:10.1029/2003JD004386.

Krawchuk MA, Moritz MA, Parisien M-A, Van Dorn J and Hayhoe K (2009) Global pyrogeography: the current and future distribution of wildfire. *PloS one*. Public Library of Science 4(4): e5102.

Lima ALC, Farrington JW and Reddy CM (2005) Combustion-derived polycyclic aromatic hydrocarbons in the environment—a review. *Environmental forensics*. Taylor & Francis 6(2): 109–131.

Malamud BD, Morein G and Turcotte DL (1998) Forest fires: an example of self-organized critical behavior. *Science*. American Association for the Advancement of Science 281(5384): 1840–1842.

Marlon JR (2020) What the past can say about the present and future of fire. *Quaternary Research*. Cambridge University Press 96: 66–87.

Marlon JR, Bartlein PJ, Gavin DG, Long CJ, Anderson RS, Briles CE, et al. (2012) Long-term perspective on wildfires in the western USA. *Proceedings of the National Academy of Sciences of the United States of America*. National Academy of Sciences 109(9): E535-43: doi:10.1073/pnas.1112839109.

McGrath TE, Chan WG and Hajaligol MR (2003) Low temperature mechanism for the formation of polycyclic aromatic hydrocarbons from the pyrolysis of cellulose. *Journal of Analytical and Applied Pyrolysis* 66(1–2): 51–70: doi:10.1016/S0165-2370(02)00105-5.

Molinari C, Carcaillet C, Bradshaw RH, Hannon GE and Lehsten V (2020) Fire-vegetation interactions during the last 11,000 years in boreal and cold temperate forests of Fennoscandia. *Quaternary Science Reviews*. Elsevier 241: 106408.

Nichols JE, Walcott M, Bradley R, Pilcher J and Huang Y (2009) Quantitative assessment of precipitation seasonality and summer surface wetness using ombrotrophic sediments from an Arctic Norwegian peatland. *Quaternary Research*. Elsevier 72(3): 443–451.

Olsson F, Gaillard M-J, Lemdahl G, Greisman A, Lanos P, Marguerie D, et al. (2010) A continuous record of fire covering the last 10,500 calendar years from southern Sweden—The role of climate and human activities. *Palaeogeography, Palaeoclimatology, Palaeoecology*. Elsevier 291(1–2): 128–141.

661 Oswald WW, Foster DR, Shuman BN, Chilton ES, Doucette DL and Duranleau DL (2020) Conservation implications of limited Native American impacts in pre-contact New England. *Nature Sustainability*. Nature Publishing Group 3(3): 241–246.

664 Pausas JG and Ribeiro E (2013) The global fire–productivity relationship. *Global Ecology and Biogeography*. Wiley Online Library 22(6): 728–736.

666 Peters ME and Higuera PE (2007) Quantifying the source area of macroscopic charcoal with a particle dispersal model. *Quaternary Research* 67(2): 304–310: doi:10.1016/j.yqres.2006.10.004.

669 Pitkänen A, Huttunen P, Jungner H and Tolonen K (2002) A 10 000 year local forest fire history in a dry heath forest site in eastern Finland, reconstructed from charcoal layer records of a small mire. *Canadian Journal of Forest Research*. NRC Research Press Ottawa, Canada 32(10): 1875–1880.

673 Reimer PJ, Austin WE, Bard E, Bayliss A, Blackwell PG, Ramsey CB, et al. (2020) The IntCal20 Northern Hemisphere radiocarbon age calibration curve (0–55 cal kBP). *Radiocarbon*. Cambridge University Press 62(4): 725–757.

676 Roos CI (2020) Scale in the study of Indigenous burning. *Nature Sustainability*. Nature Publishing Group 3(11): 898–899.

678 Sjögren P and Arntzen JE (2013) Agricultural practices in Arctic Norway during the first millennium BC. *Vegetation History and Archaeobotany*. Springer 22(1): 1–15.

680 Stuiver M and Reimer PJ (1993) Extended 14C data base and revised CALIB 3.0 14C age calibration program. *Radiocarbon*. Cambridge University Press 35(1): 215–230.

682 Tan Z, Wu C, Han Y, Zhang Y, Mao L, Li D, et al. (2020) Fire history and human activity revealed through poly cyclic aromatic hydrocarbon (PAH) records at archaeological sites in the middle reaches of the Yellow River drainage basin, China. *Palaeogeography, Palaeoclimatology, Palaeoecology*. Elsevier 560: 110015.

686 Tingley MT (2022) Pollen Evidence of Late Holocene Human-Landscape Impact in the Lofoten Islands, Norway. Northern Arizona University.

688 Tryterud E (2003) Forest fire history in Norway: from fire-disturbed pine forests to fire-free spruce forests. *Ecography*. Wiley Online Library 26(2): 161–170.

690 Turcotte DL and Malamud BD (2004) Landslides, forest fires, and earthquakes: examples of self-organized critical behavior. *Physica A: Statistical Mechanics and its Applications*. Elsevier 340(4): 580–589.

693 Utne A (1973) En veidekulturs-boplass i Lofoten. *Storbåthallaren ved Nappstraumen. Bd* 1.

Vachula RS (2021) A meta-analytical approach to understanding the charcoal source area problem. *Palaeogeography, Palaeoclimatology, Palaeoecology*. Elsevier 562: 110111: doi:10.1016/j.palaeo.2020.110111.

Vachula RS, Karp AT, Denis EH, Balascio NL, Canuel EA and Huang Y (2022) Spatially calibrating polycyclic aromatic hydrocarbons (PAHs) as proxies of area burned by vegetation fires: Insights from comparisons of historical data and sedimentary PAH fluxes. *Palaeogeography, Palaeoclimatology, Palaeoecology*. Elsevier 110995.

Vachula RS and Richter N (2018) Informing sedimentary charcoal-based fire reconstructions with a kinematic transport model. *Holocene*. SAGE PublicationsSage UK: London, England 28(1): 173–178: doi:10.1177/0959683617715624.

Vachula RS, Russell JM and Huang Y (2019) Climate exceeded human management as the dominant control of fire at the regional scale in California's Sierra Nevada. *Environmental Research Letters* 14(10): doi:10.1088/1748-9326/ab4669.

Vachula RS, Russell JM, Huang Y and Richter N (2018) Assessing the spatial fidelity of sedimentary charcoal size fractions as fire history proxies with a high-resolution sediment record and historical data. *Palaeogeography, Palaeoclimatology, Palaeoecology*. Elsevier B.V. 508: 166–175: doi:10.1016/j.palaeo.2018.07.032.

Vachula RS, Sae-Lim J and Russell JM (2020) Sedimentary charcoal proxy records of fire in Alaskan tundra ecosystems. *Palaeogeography, Palaeoclimatology, Palaeoecology* 541: doi:10.1016/j.palaeo.2019.109564.

Vorren K (1979) Anthropogenic influence on the natural vegetation in coastal North Norway during the Holocene. Development of farming and pastures. *Norwegian Archaeological Review*. Taylor & Francis 12(1): 1–21.

Vorren K-D, Jensen CE and Nilssen E (2012) Climate changes during the last c. 7500 years as recorded by the degree of peat humification in the Lofoten region, Norway. *Boreas*. Wiley Online Library 41(1): 13–30.

Whitlock C and Larsen C (2002) Charcoal as a Fire Proxy. *Tracking Environmental Change Using Lake Sediments*. Dordrecht: Kluwer Academic Publishers, 75–97: doi:10.1007/0-306-47668-1_5.

Table 1. Radiocarbon sample information for records from Inner Borgpollen, Ostadvatnet, and Lauvdalsvatnet. All radiocarbon ages are from terrestrial plant remains and calibrated using the IntCal20 calibration curve (Reimer et al., 2020).

Site	Laboratory ID[a]	Composite Depth (cm)	Sample Name	Radiocarbon Age (yr BP)	Calibrated Age Range (yr BP, 2σ)	Median Age (cal yr BP)
Inner Borgpollen	UCI-239585	34-34.5	IND-01-17 1/2	430 ± 25	343-524	498
	UCI-191997	56-58	IND-01-17 1/2	1340 ± 15	1179-1298	1285
	UCI-204833	78-79	IND-01-17 1/2	1840 ± 20	1707-1821	1738
	UCI-191998	96-97	IND-01-17 1/2	2335 ± 15	2338-2355	2348
	UCI-204834	133-134	IND-01-17 2/2	2860 ± 110	2758-3324	3001
	UCI-191999	172-173	IND-01-17 2/2	3200 ± 15	3383-3451	3419
Ostadvatnet	OS-135766	23-23.5	OSD-01-17	2010 ± 15	1890-1994	1957
	UCI-191994	51.5-52.5	OSD-01-18	2890 ± 15	2958-3134	3020
	UCI-191993	111.5-112	OSD-01-19	4425 ± 20	4876-5264	5007
Lauvdalsvatnet	OS-135762	41.4-42.4	LVP-01-17 1/2	1330 ± 15	1178-1295	1279
	UCI-204831	85.7-86.7	LVP-01-17 1/2	2290 ± 15	2183-2348	2334
	OS-135763	114.9-115.9	LVP-01-17 1/2	3110 ± 20	3249-3382	3337
	UCI-204832	160.3-161.3	LVP-01-17 2/2	3910 ± 20	4253-4416	4353
	OS-135764	179.9-180.9	LVP-01-17 2/2	4530 ± 25	5051-5312	5155
	OS-135765	222.2-223.2	LVP-01-17 2/2	6280 ± 25	7162-7259	7214

[a] *UCI* - University of California Irvine Keck-CCAMS Facility; *OS* - National Ocean Sciences AMS Facility

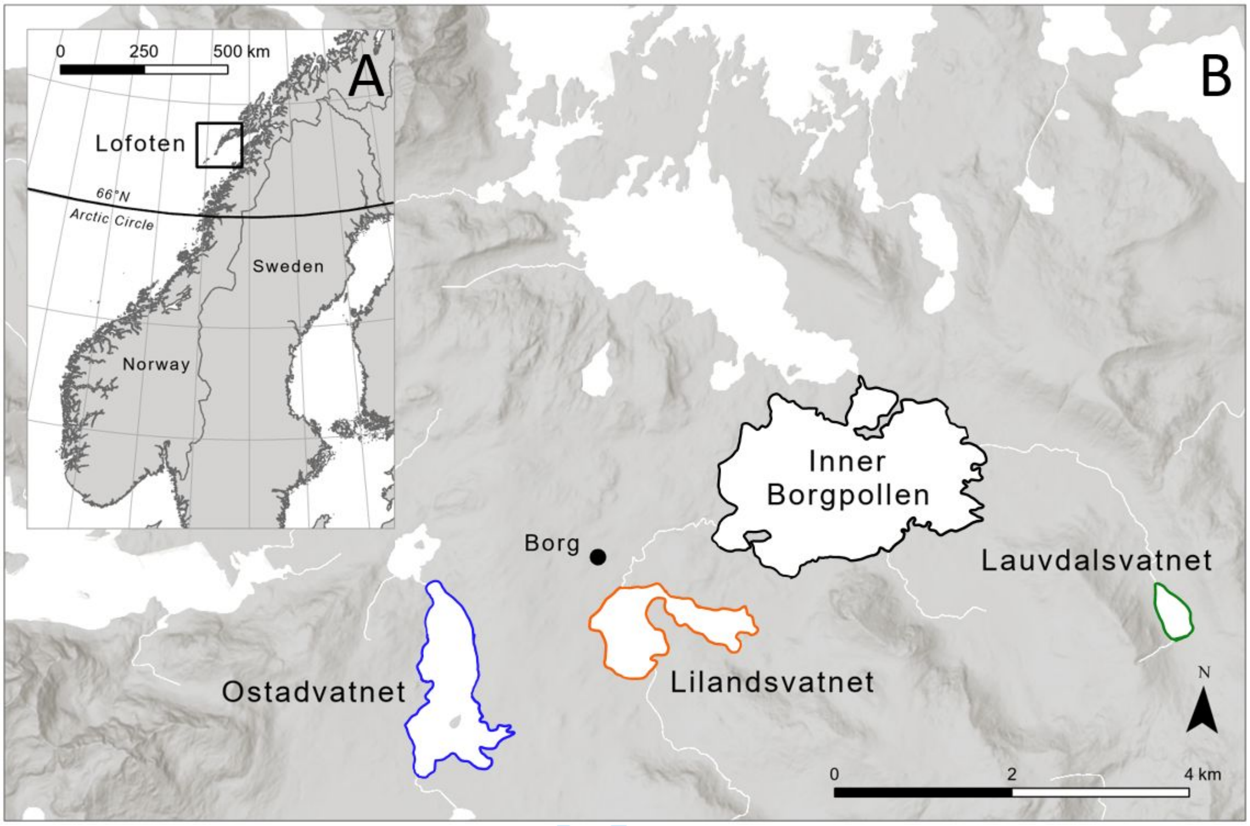

Figure 1. (A) Map of the Lofoten Islands off the coast of northern Norway. (B) Location of lakes Ostadvatnet (blue outline), Inner Borgpollen (black outline), and Lauvdalsvatnet (green outline) on Vestvågøya. Lilandsvatnet (orange outline) is also shown. Iron Age settlement at Borg indicated with black dot. Base map sources: Esri; Garmin International, Inc. and Copernicus; European Environment Agency.

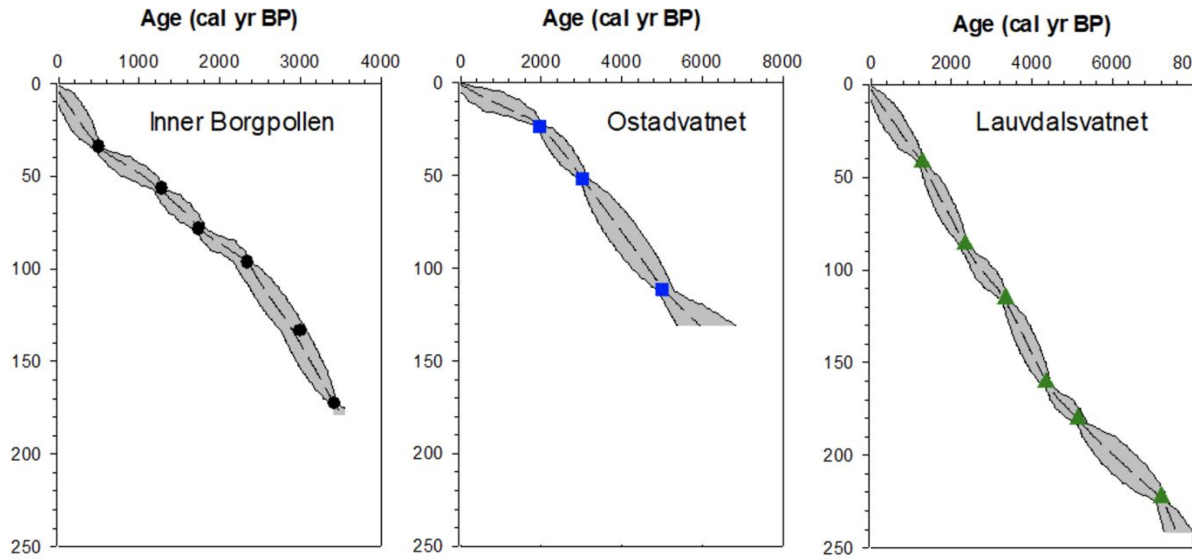

Figure 2. Radiocarbon ages (Table 1) and age-depth models generated using the Bacon age modelling software (Blauuw and Christen, 2011) for records from Lauvdalsvatnet, Ostadvatnet, and Inner Borgpollen. Gray area shows 95% confidence intervals around median ages (dashed line) for each record.

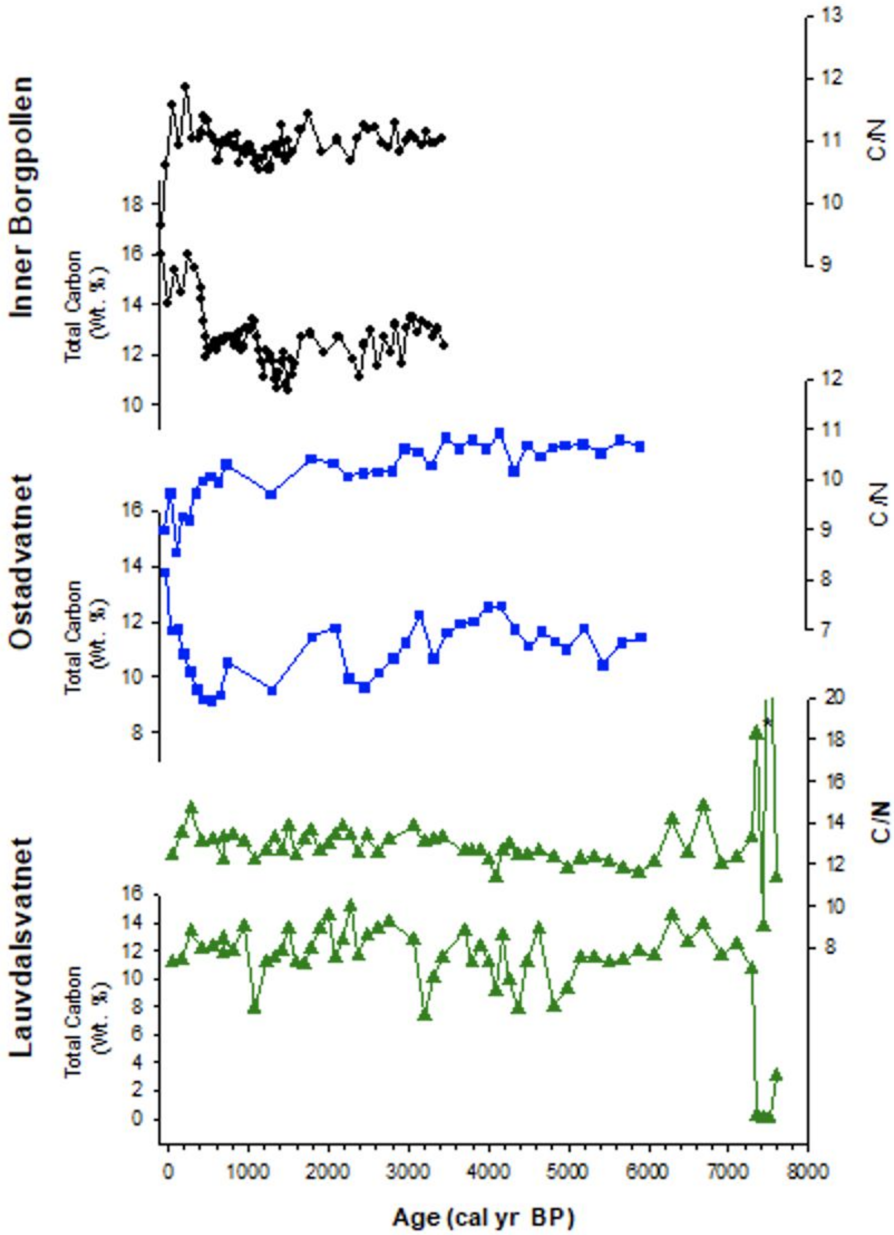

Figure 3. Total carbon and carbon/nitrogen (C/N) profiles for Inner Borgpollen (black circles), Ostadvatnet (blue squares), and Lauvdalsvatnet (green triangles).

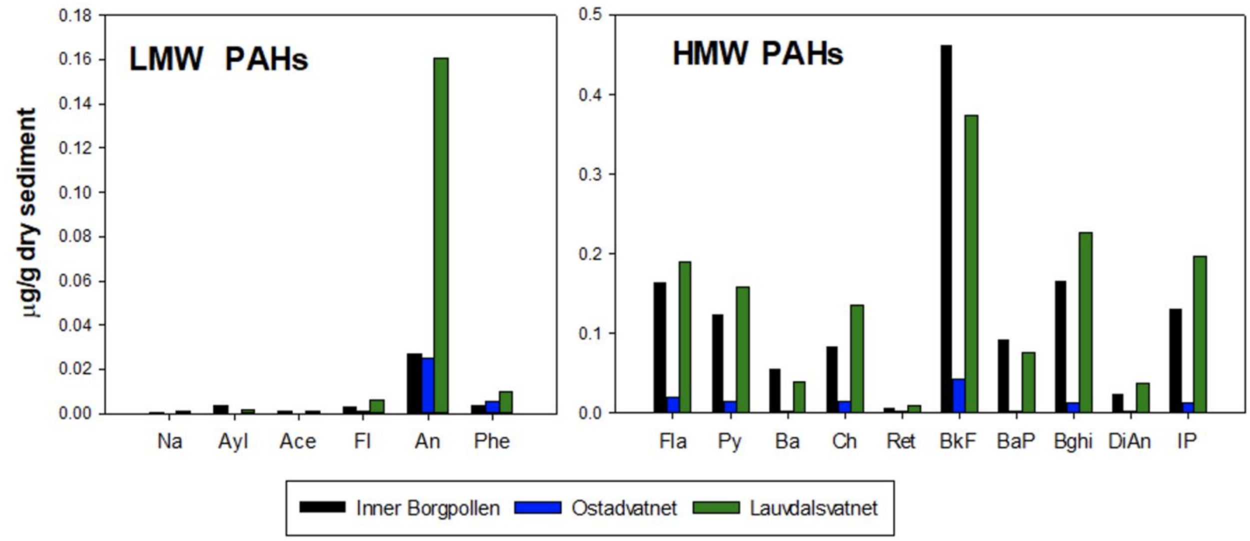

Figure 4. Total concentrations of low molecular weight (LMW) and high molecular weight (HMW) PAHs in samples analyzed from Inner Borgpollen, Ostadvatnet, and Lauvdalsvatnet. Compounds include: naphthalene (Na), acenaphthylene (Ayl), acenaphthene (Ace), fluorene (Fl), anthracene (An), phenanthrene (Phe), fluoranthene (Fla), pyrene (Py), benz[a]anthrene (Ba), chrysene (Ch), retene (Ret), benzo[k]fluoranthene (BkF), benzo[a]pyrene (BaP), benzo[g,h,i]perylene (Bghi), dibenzo[a,h]anthracene (DiAn), and ideno[1,2,3-cd]pyrene (IP).

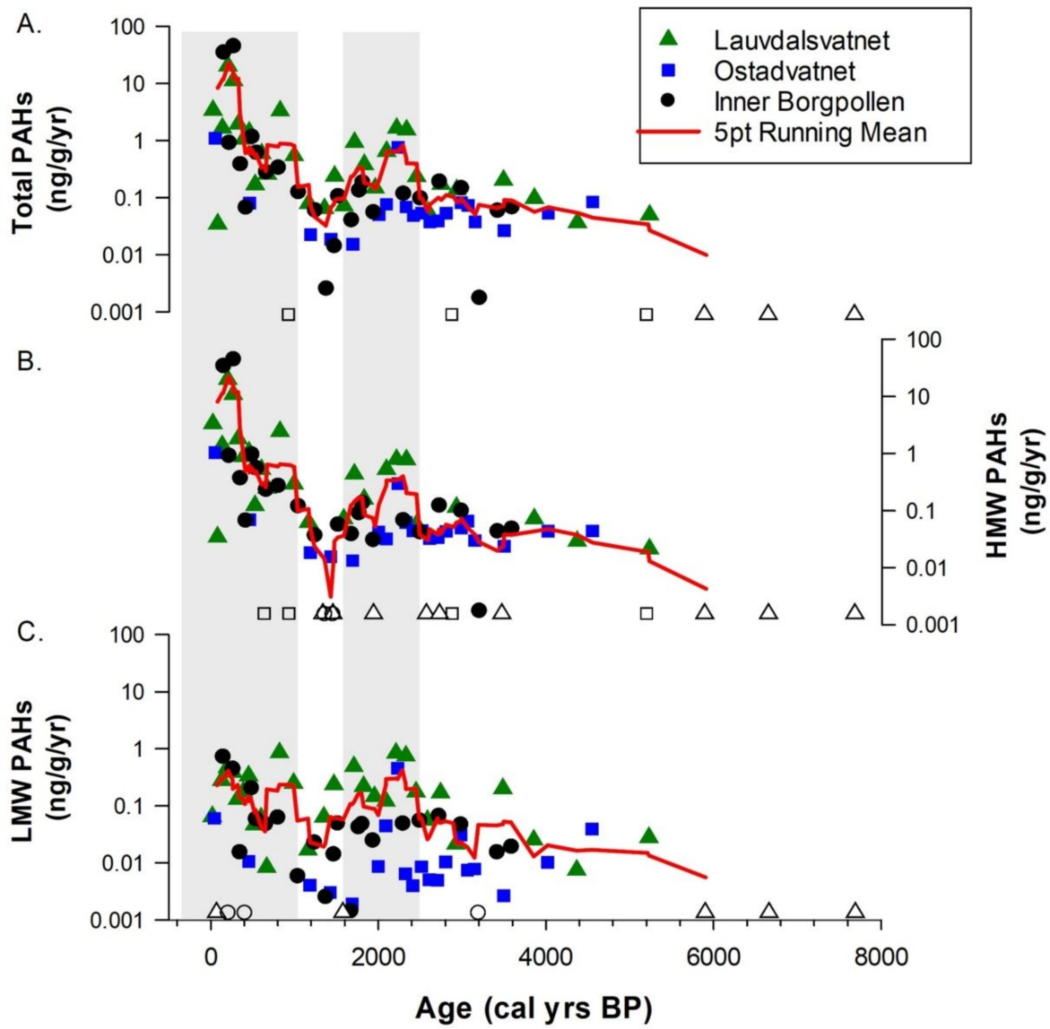

Figure 5. (A.) Total PAH records for Lauvdalsvatnet, Ostadvatnet, and Inner Borgpollen showing changes in the accumulation rate of 16 PAHs over the last c. 7500 cal yr BP and a five-point running mean through all samples. Also shown are: (B.) trends in high molecular weight (HMW), and (C.) low molecular weight (LMW) PAHs for each site. Open symbols indicate samples below detection limits. Shaded areas mark intervals of high accumulation rates c. 2400-1500 cal yr BP and 900 cal yr BP to present. Null values and/or samples with PAH concentrations under the detection limit are not plotted due to the logarithmic axes.

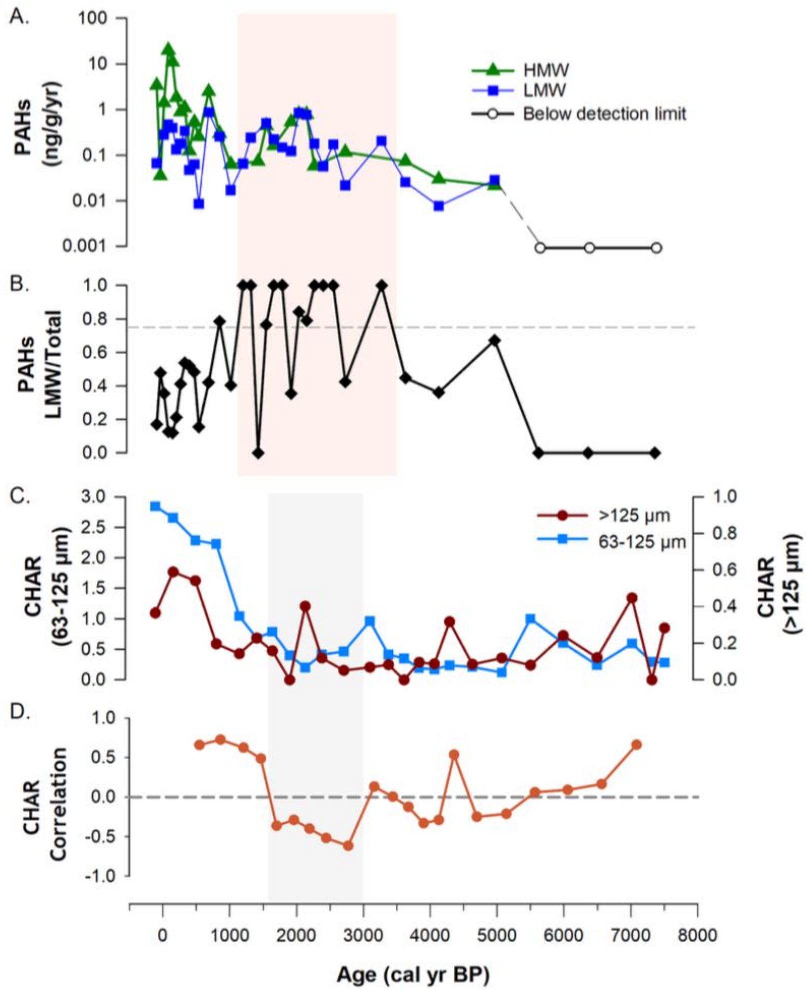

Figure 6. PAH and charcoal data from Lauvdalsvatnet. (A.) High molecular weight (HMW) and low molecular weight (LMW) PAH accumulation rates. (B.) LMW accumulation rates relative to total PAHs. Pink shading marks interval where LMW/Total values exceed 0.75 (dashed line), which we interpret to reflect inputs of PAHs derived from smoke phases relative to a dominance of PAHs derived from combustion residues (<0.75) in the rest of the record (Karp et al., 2020). (C.) Charcoal accumulation rates (CHAR) for particles >125 µm and 63-125 µm. (D.) Correlation between CHAR >125 µm and CHAR 125-63 µm shown as a 5-point moving average. Gray shading marks interval where CHAR correlation values are consistently negative from c. 3000 to 1500 cal yr BP.

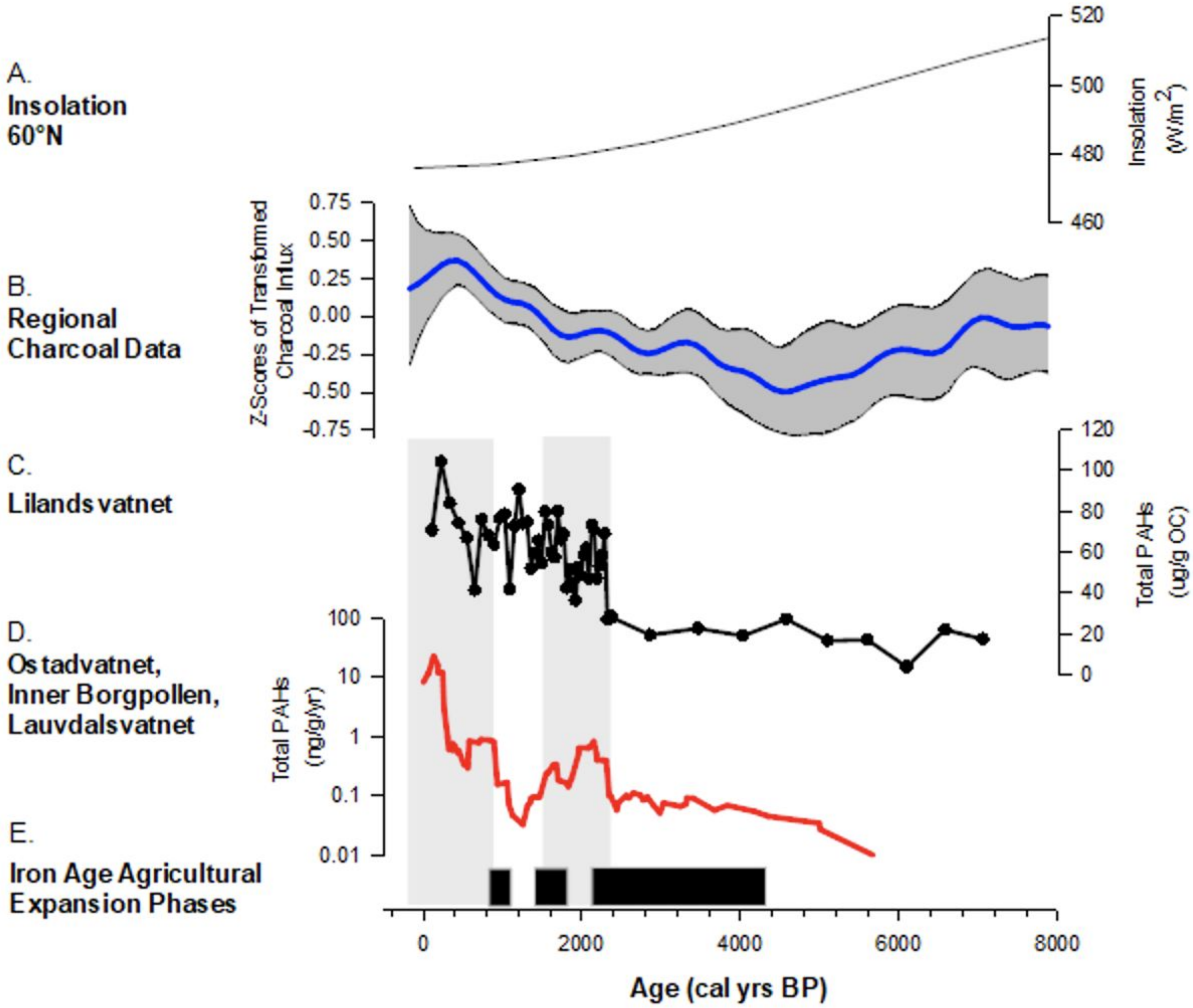

Figure 7. Comparison of (A.) June insolation at 60°N (Berger and Loutre, 1991), (B.) compilation of regional charcoal records from Fennoscandia (gray lines indicate 95% confidence interval) (Molinari et al., 2020), (C.) total PAH data from Lilandsvatnet (D'Anjou et al., 2012), (D.) five-point running mean of total PAH data from Ostadvatnet, Inner Borgpollen, and (E.) Iron Age agricultural expansion phases (Sjögren and Arntzen, 2013). Shaded areas mark intervals of high accumulation rates in records from this study, c. 2400-1500 cal yr BP and 900 cal yr BP to present.

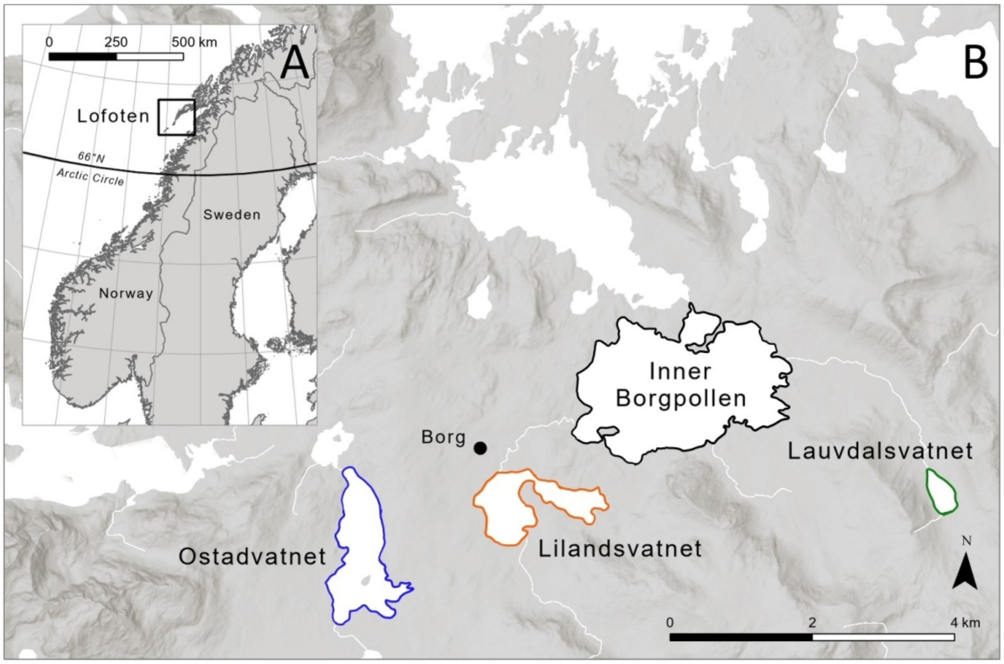

Figure 1. (A) Map of the Lofoten Islands off the coast of northern Norway. (B) Location of lakes Ostadvatnet (blue outline), Inner Borgpollen (black outline), and Lauvdalsvatnet (green outline) on Vestvågøya. Lilandsvatnet (orange outline) is also shown. Iron Age settlement at Borg indicated with black dot. Base map sources: Esri; Garmin International, Inc. and Copernicus; European Environment Agency.

267x175mm (144 x 144 DPI)

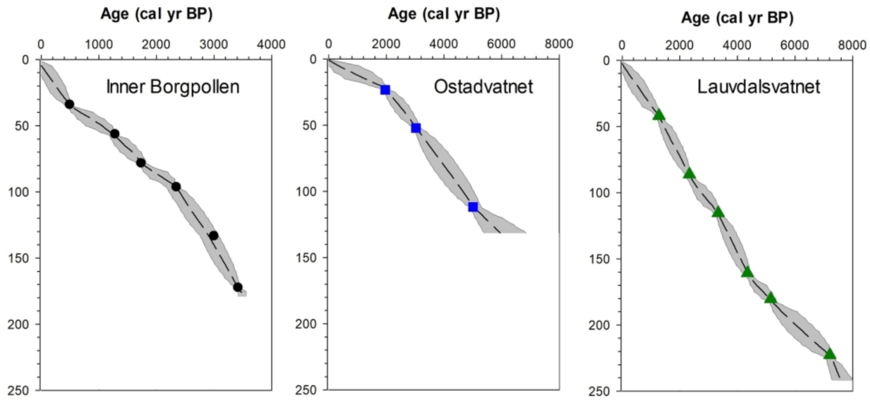

Figure 2. Radiocarbon ages (Table 1) and age-depth models generated using the Bacon age modelling software (Blauuw and Christen, 2011) for records from Lauvdalsvatnet, Ostadvatnet, and Inner Borgpollen. Gray area shows 95% confidence intervals around median ages (dashed line) for each record.

158x80mm (300 x 300 DPI)

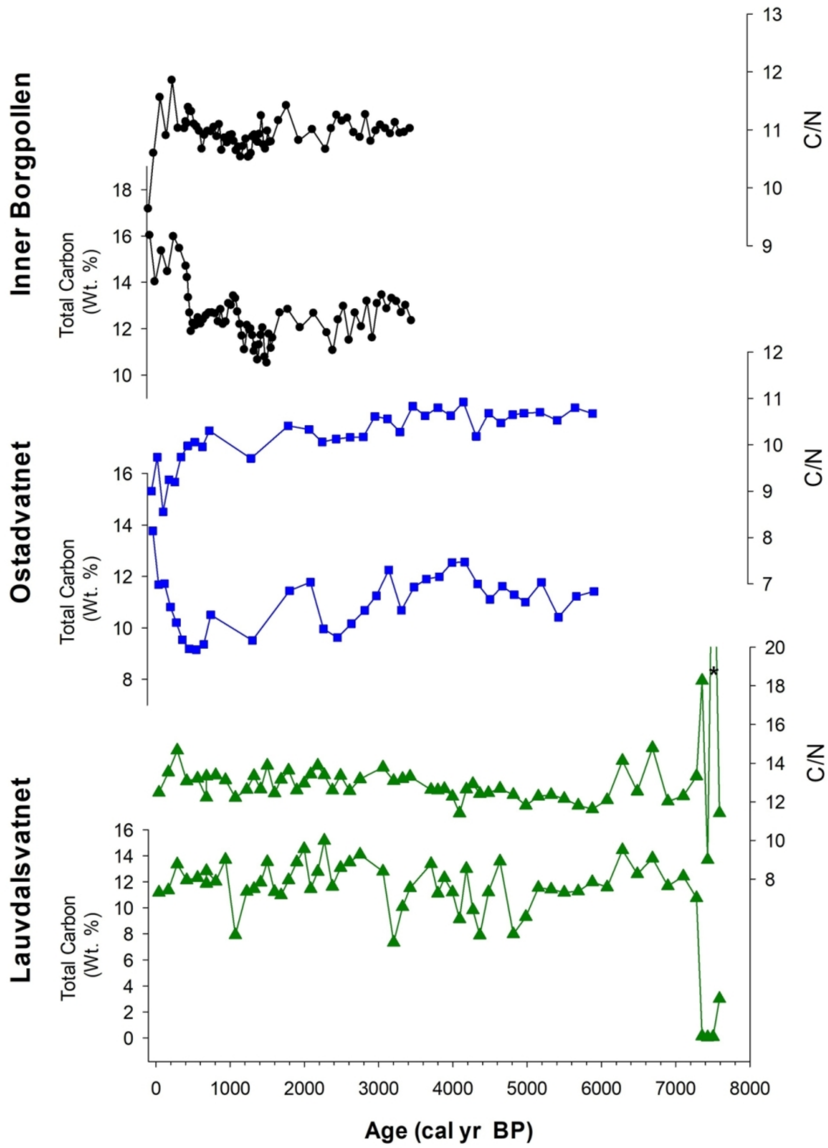

Figure 3. Total carbon and carbon/nitrogen (C/N) profiles for Inner Borgpollen (black circles), Ostadvatnet (blue squares), and Lauvdalsvatnet (green triangles).

120x156mm (300 x 300 DPI)

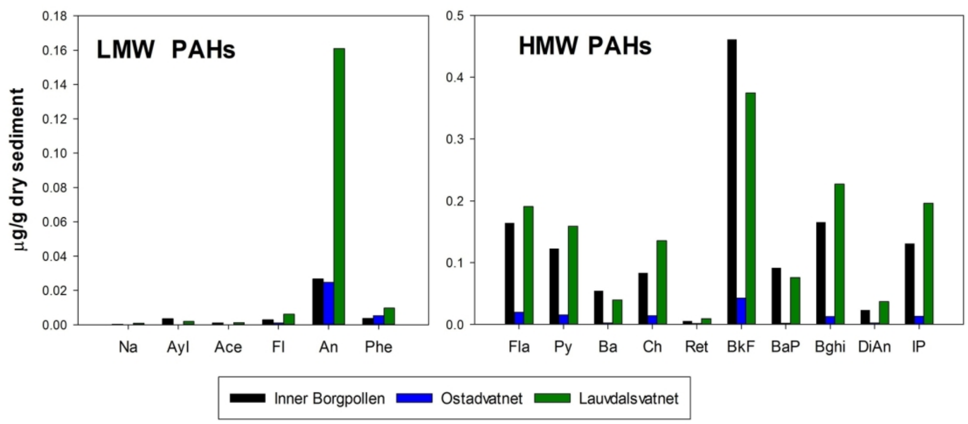

Figure 4. Total concentrations of low molecular weight (LMW) and high molecular weight (HMW) PAHs in samples analyzed from Inner Borgpollen, Ostadvatnet, and Lauvdalsvatnet. Compounds include: naphthalene (Na), acenaphthylene (Ayl), acenaphthene (Ace), fluorene (Fl), anthracene (An), phenanthrene (Phe), fluoranthene (Fla), pyrene (Py), benz[a]anthrene (Ba), chrysene (Ch), retene (Ret), benzo[k]fluoranthene (BkF), benzo[a]pyrene (BaP), benzo[g,h,i]perylene (Bghi), dibenzo[a,h]anthracene (DiAn), and ideno[1,2,3-cd]pyrene (IP).

158x80mm (300 x 300 DPI)

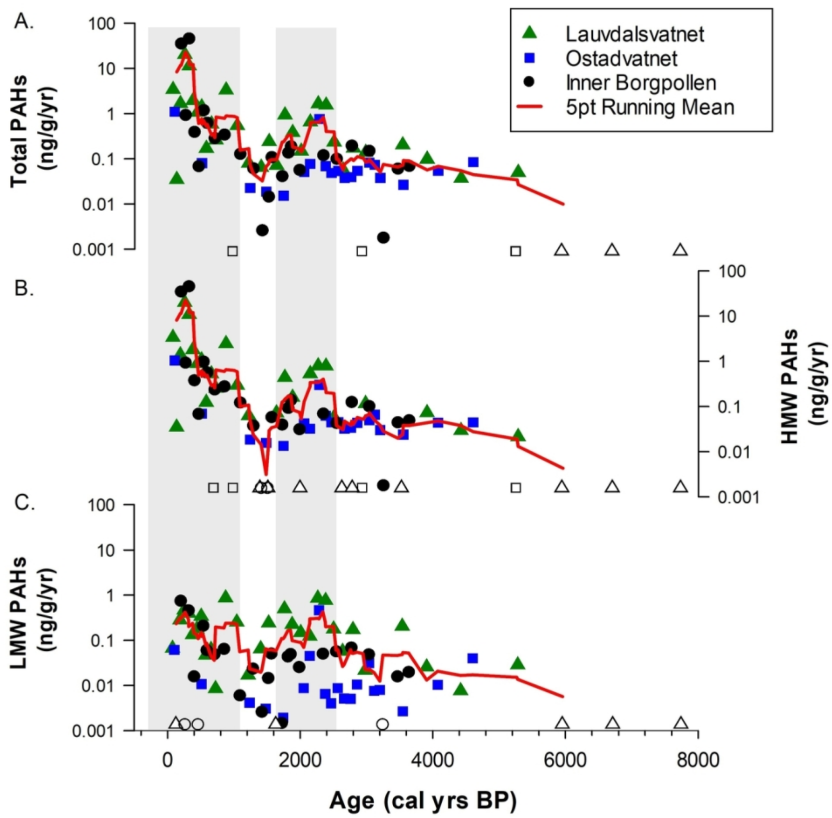

Figure 5. (A.) Total PAH records for Lauvdalsvatnet, Ostadvatnet, and Inner Borgpollen showing changes in the accumulation rate of 16 PAHs over the last c. 7500 cal yr BP and a five-point running mean through all samples. Also shown are: (B.) trends in high molecular weight (HMW), and (C.) low molecular weight (LMW) PAHs for each site. Open symbols indicate samples below detection limits. Shaded areas mark intervals of high accumulation rates c. 2400-1500 cal yr BP and 900 cal yr BP to present. Null values and/or samples with PAH concentrations under the detection limit are not plotted due to the logarithmic axes.

140x132mm (300 x 300 DPI)

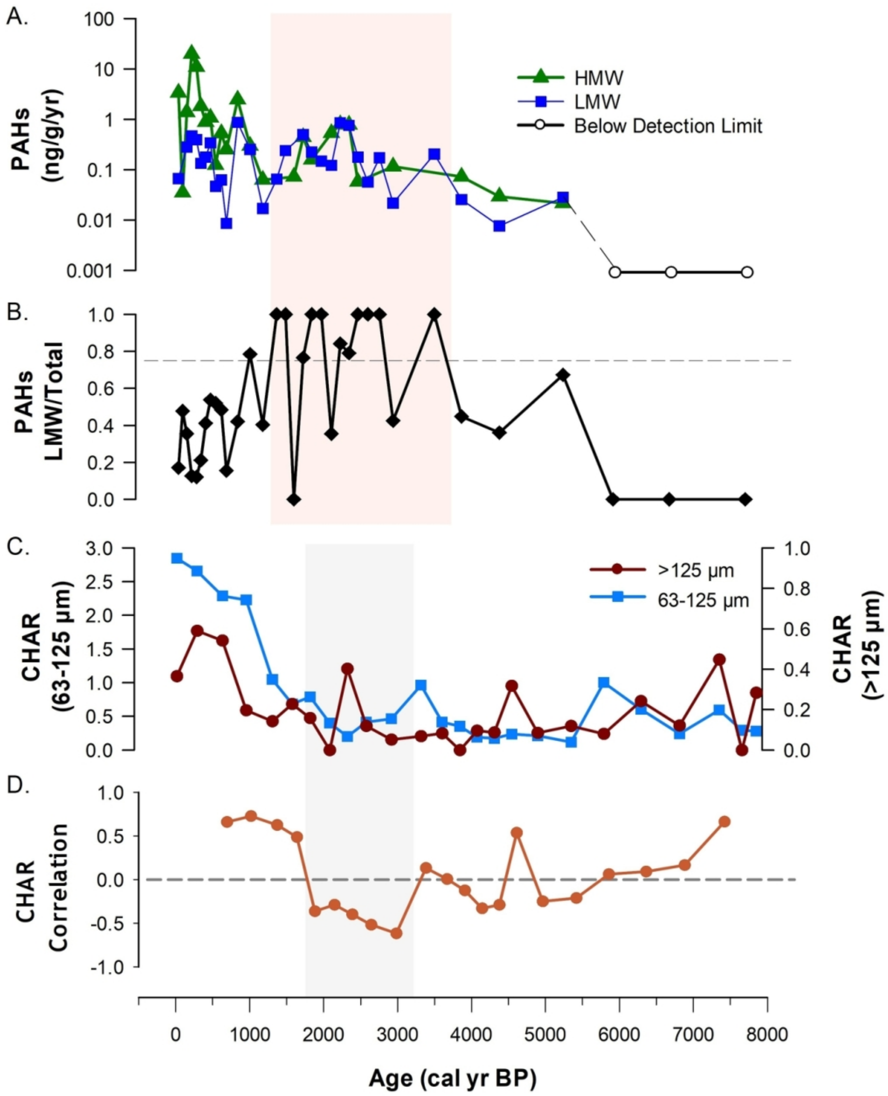

Figure 6. PAH and charcoal data from Lauvdalsvatnet. (A.) High molecular weight (HMW) and low molecular weight (LMW) PAH accumulation rates. (B.) LMW accumulation rates relative to total PAHs. Pink shading marks interval where LMW/Total values exceed 0.75 (dashed line), which we interpret to reflect inputs of PAHs derived from smoke phases relative to a dominance of PAHs derived from combustion residues (<0.75) in the rest of the record (Karp et al., 2020). (C.) Charcoal accumulation rates (CHAR) for particles >125 µm and 63-125 µm. (D.) Correlation between CHAR >125 □m and CHAR 125-63 □m shown as a 5-point moving average. Gray shading marks interval where CHAR correlation values are consistently negative from c. 3000 to 1500 cal yr BP.

126x145mm (300 x 300 DPI)

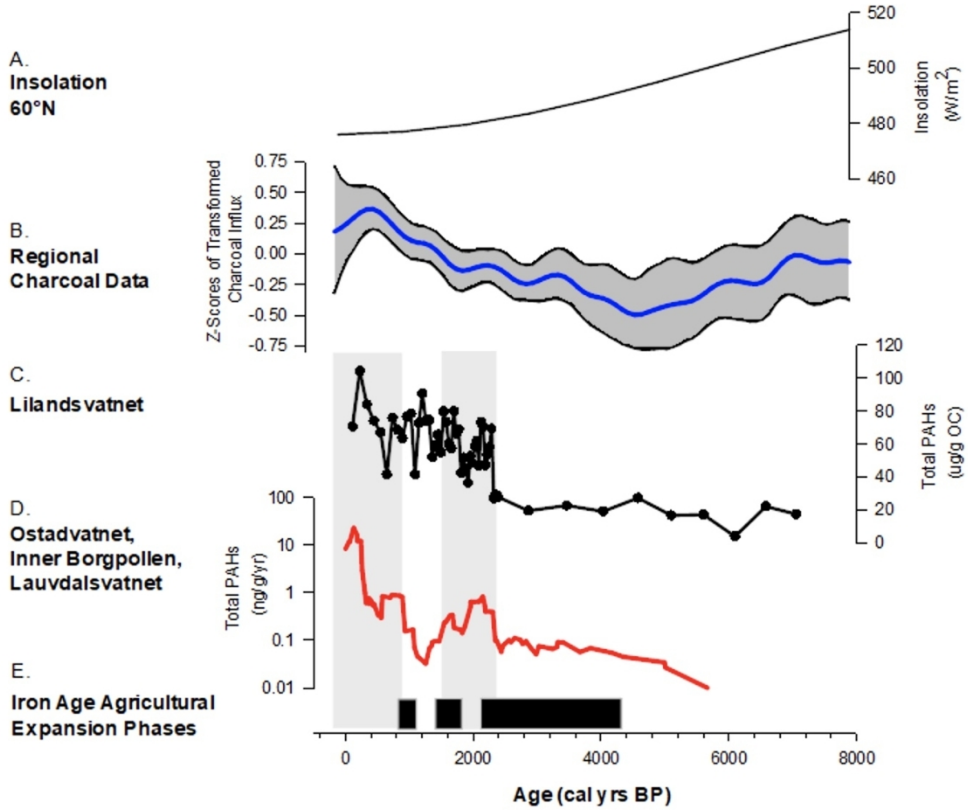

Figure 7. Comparison of (A.) June insolation at 60°N (Berger and Loutre, 1991), (B.) compilation of regional charcoal records from Fennoscandia (gray lines indicate 95% confidence interval) (Molinari et al., 2020), (C.) total PAH data from Lilandsvatnet (D'Anjou et al., 2012), (D.) five-point running mean of total PAH data from Ostadvatnet, Inner Borgpollen, and (E.) Iron Age agricultural expansion phases (Sjögren and Arntzen, 2013). Shaded areas mark intervals of high accumulation rates in records from this study, c. 2400-1500 cal yr BP and 900 cal yr BP to present.

245x208mm (144 x 144 DPI)

Table X. Radiocarbon sample information for sediment core records from Inner Borgpollen, Ostadvatnet, and Lauvdalsvatnet. All radiocarbon ages are from terrestrial plant remains picked from the cores and calibrated ages are based on the IntCal20 calibration curve (Reimer et al., 2020).

Site	Laboratory ID[a]	Composite Depth (cm)	Sample Name	Radiocarbon Age (yr BP)	Calibrated Age Range (yr BP, 2σ)	Median Age (cal yr BP)
Inner Borgpollen	UCI-239585	34-34.5	IND-01-17 1/2	430 ± 25	343-524	500
	UCI-191997	56-58	IND-01-17 1/2	1340 ± 15	1179-1298	1290
	UCI-204833	78-79	IND-01-17 1/2	1840 ± 20	1707-1821	1740
	UCI-191998	96-97	IND-01-17 1/2	2335 ± 15	2338-2355	2350
	UCI-204834	133-134	IND-01-17 2/2	2860 ± 110	2758-3324	3000
	UCI-191999	172-173	IND-01-17 2/2	3200 ± 15	3383-3451	3420
Ostadvatnet	OS-135766	23-23.5	OSD-01-17	2010 ± 15	1890-1994	1957
	UCI-191994	51.5-52.5	OSD-01-18	2890 ± 15	2958-3194	3020
	UCI-191993	111.5-112	OSD-01-19	4425 ± 20	4876-5264	5007
Lauvdalsvatnet	OS-135762	41.4-42.4	LVP-01-17 1/2	1330 ± 15	1178-1295	1279
	UCI-204831	85.7-86.7	LVP-01-17 1/2	2290 ± 15	2183-2348	2334
	OS-135763	114.9-115.9	LVP-01-17 1/2	3110 ± 20	3249-3382	3337
	UCI-204832	160.3-161.3	LVP-01-17 2/2	3910 ± 20	4253-4416	4353
	OS-135764	179.9-180.9	LVP-01-17 2/2	4530 ± 25	5051-5312	5155
	OS-135765	222.2-223.2	LVP-01-17 2/2	6280 ± 25	7162-7259	7214

[a] *UCI* - University of California Irvine Keck-CCAMS Facility; *OS* - National Ocean Sciences AMS Facility